Journal of Hydrology 400 (2011) 83–94

Contents lists available at ScienceDirect

Journal of Hydrology

journal homepage: www.elsevier.com/locate/jhydrol

Rainfall uncertainty in hydrological modelling: An evaluation of multiplicative error models

Hilary McMillan[a,*], Bethanna Jackson[b], Martyn Clark[a], Dmitri Kavetski[c], Ross Woods[a]

[a] National Institute of Water and Atmospheric Research, Christchurch, New Zealand
[b] School of Geography, Environment and Earth Sciences, Victoria University of Wellington, New Zealand
[c] School of Engineering, University of Newcastle, Callaghan, Australia

ARTICLE INFO

Article history:
Received 5 August 2010
Received in revised form 18 January 2011
Accepted 21 January 2011
Available online 27 January 2011

This manuscript was handled by A. Bardossy, Editor-in-Chief, with the assistance of Attilio Castellarin, Associate Editor

Keywords:
Hydrology
Rainfall
Radar
Error models
Input uncertainty

SUMMARY

This paper presents an investigation of rainfall error models used in hydrological model calibration and prediction. Traditional calibration methods assume input error to be negligible: an assumption which can lead to bias in parameter estimation and compromise model predictions. In response, a growing number of studies now specify an error model for rainfall input, usually simple in form due to both difficulties in understanding sampling errors in rainfall, and to computational constraints during parameter estimation. Such rainfall error models have not typically been validated against experimental evidence. In this study we use data from a dense gauge/radar network in the Mahurangi catchment (New Zealand) to directly evaluate the form of basic statistical rainfall error models. For this catchment, our results confirm the suitability of a multiplicative error formulation for correcting mean catchment rainfall values during high-rainfall periods (e.g., intensities over 1 mm/h); or for longer timesteps at any rainfall intensity (timestep 1 day or greater). We show that the popular lognormal multiplier distribution provides a relatively close approximation to the true error characteristics but does not capture the distribution tails, especially during heavy rainfall where input errors would have important consequences for runoff prediction. Our research highlights the dependency of rainfall error structure on the data timestep.

1. Introduction

Adequate characterization of rainfall inputs is fundamental to success in rainfall–runoff modelling: no model, however well-founded in physical theory or empirically justified by past performance, can produce accurate runoff predictions if forced with inaccurate rainfall data (e.g., Beven, 2004). The impact of rainfall errors on predicted flow has been highlighted by many authors, including Sun et al. (2000), Kavetski et al. (2002, 2006a), Bárdossy and Das (2008), and Moulin et al. (2009). From a management perspective, inaccuracies in rainfall inputs directly compromise model predictions and hence also compromise robust decision-making on water and risk management options. An accurate statistical representation of rainfall errors has potential for real-time bias correction and uncertainty estimation of streamflow forecasts. Furthermore, errors in rainfall reduce our ability to identify other sources of error and uncertainty, slowing scientific advancement and compromizing the reliability of operational applications. This issue is recognized as a major challenge for hydrological modelling science (Kuczera et al., 2006).

The impact of input uncertainty on streamflow simulations can be quantified by error propagation, either by using conditional simulation or simply by stochastically perturbing the rainfall inputs. Conditional simulation involves generating ensemble rainfall fields conditioned on the mean and error of spatial rainfall interpolations (e.g., Clark and Slater, 2006; Gotzinger and Bardossy, 2008). Conditional simulation methods may provide a better description of rainfall errors (e.g., Clark and Slater, 2006), but can be data-intensive to parameterize and computationally expensive to run. Stochastic perturbation of rainfall inputs is therefore more common (Reichle et al., 2002; Carpenter and Georgakakos, 2004; Crow and van Loon, 2006; Pauwels and de Lannoy, 2006; Komma et al., 2008; Pan et al., 2008; Turner et al., 2008).

In the stochastic perturbation approach it is common to perturb the model rainfall inputs based only on order of magnitude considerations. For example, Reichle et al. (2002) used perturbations with standard deviation equal to 50% of the rainfall total at each model timestep. Given that uncertainty in hydrological simulations directly depends on adequate characterization of input error (e.g., Crow and van Loon, 2006; Gotzinger and Bardossy, 2008; Renard et al., 2010), detailed analysis of the observed error of rainfall inputs is a critical research priority: estimating rainfall errors based only on order of magnitude considerations can no longer be justified.

* Corresponding author. Tel.: +64 33438071.
E-mail address: h.mcmillan@niwa.co.nz (H. McMillan).

0022-1694/$ - see front matter © 2011 Elsevier B.V. All rights reserved.
doi:10.1016/j.jhydrol.2011.01.026

This paper directly evaluates rainfall error models that are commonly used in rainfall–runoff model calibration and prediction. Research is based on the 50 km^2 Mahurangi catchment in Northland, New Zealand where there is detailed space–time information on rainfall from both a dense gauge network (13 stations) and high-resolution radar rainfall estimates. This dataset provides a valuable opportunity to evaluate basic statistical rainfall error models. Our main focus is on understanding uncertainties in raingauge network measurements, since they remain the most common source of rainfall measurements. We consider total uncertainty, i.e., the combination of sampling (interpolation) error together with measurement error, although sampling error would be expected to dominate at the spatial scales in question. We also provide a comparative analysis based on available high-resolution radar fields, to enhance our understanding of the spatial/temporal rainfall variability and its effects on rainfall uncertainty at both the distributed and point scale, in space and in time. We aim to provide practical guidance on the temporal scales at which multiplicative error models with various distributions and parameterisations might be appropriate. Our broader objective is to contribute independent information and guidance to ongoing work on quantifying the impact of errors and uncertainties in rainfall on the quality of calibrated parameters and/or on streamflow estimates (Carpenter and Georgakakos, 2004; Bárdossy and Das, 2008; Thyer et al., 2009; Moulin et al., 2009; Kavetski et al., 2006b; Ajami et al., 2007; Vrugt et al., 2003b).

2. Sources of rainfall input uncertainty in hydrological models

When using raingauge data, as is currently common in hydrological modelling, a major source of uncertainty arises from "sampling error" caused by (i) inadequacies in the representation of the precipitation field over the entire catchment by a (typically small) set of point-scale gauges (Refsgaard et al., 2006; Villarini et al., 2008; Moulin et al., 2009; Volkmann et al., 2010), and (ii) the assumptions used to interpolate rain rates between these gauges. Bras and Rodriguez-Iturbe (1976) showed the importance of raingauge network design for estimation of areal mean rainfall. Additional uncertainty is introduced via "measurement error": the commonly used tipping bucket raingauges are subject to both systematic and random errors, with mechanical limitations, wind effects and evaporation losses (Molini et al., 2001; la Barbera et al., 2002; Shedekar et al., 2009). Measurement errors are themselves dependent on rainfall intensity and timescale (Habib et al., 2001; Ciach, 2003).

In contrast to the generally sparse raingauge networks, radar offers the potential of providing integrated rainfall estimates over large spatial areas. Weather radar coverage has dramatically increased over the last few decades, giving access to measurements at high spatial and temporal resolutions (Moulin et al., 2009). Although signal treatment methods have significantly improved (Krajewski and Smith, 2002; Chapon et al., 2008), conversion of raw radar data into quantitative precipitation estimates still presents significant difficulties. Errors are primarily related to the non-uniform vertical profile of reflectivity, drifts in the radar calibration constant and biased reflectivity-to-rainrate (Z–R) relationship (Villarini and Krajewski, 2010); these have often precluded the use of standalone radar estimates for runoff modelling (Borga, 2002).

The field of radar meteorology offers useful insights into the space–time error characteristics of radar precipitation estimates. Early theoretical work related error variance to sampling interval, sampling period, spatial averaging area and rain rate (North, 1987). At longer timescales, Steiner (1996) and Steiner et al. (2003) used raingauge networks and radar data to estimate the effect of space and time domain, sampling frequency, and rainfall characteristics on uncertainty of areal rainfall estimates for accumulations of 1–30 days. Errors in spatial statistics (Gebremichael and Krajewski, 2005) and rain rates (Bell and Kundu, 2000; Gebremichael and Krajewski, 2004) estimated using radar data have also been investigated. A review of errors in radar rainfall space–time averages is provided by Astin (1997). At larger scales than those relating to rainfall radar, satellite estimates of rainfall may be used, and bring their own set of error characteristics and estimation methods (Hossain and Anagnostou, 2005a,b; Hossain and Huffman, 2008).

It is increasingly recognized that uncertainty in rainfall has a critical effect on the accuracy of hydrological model predictions, and that efforts to advance scientific understanding through using streamflow data to evaluate hydrological model parameters and structural hypotheses are hampered by errors and incorrect assumptions regarding the quality of the rainfall used to drive the hydrological model. In the recent study of Reichert and Mieleitner (2009), allowing time dependency in rainfall bias improved model performance more than inclusion of any other time dependent parameter, while in the studies of Wagener et al. (2007) and Yatheendradas et al. (2008), depth biases in rainfall estimates almost completely dominated the errors in runoff predictions. Kavetski et al. (2006a) note that despite advances in data collection and model construction, the high spatial and temporal variability of precipitation make it probable that rainfall input uncertainty will remain considerable in the foreseeable future.

3. Error models for rainfall measurements

All methods used to calibrate hydrological models are based on hypotheses and assumptions, either explicit or implicit, describing how errors arise and propagate through a hydrological system (Kavetski et al., 2002). In traditional calibration, such as standard least squares (SLS) and equivalent methods based on the Nash–Sutcliffe optimization, input error is assumed negligible and the model and response errors are represented as an additive random process (Kavetski et al., 2002; Kuczera et al., 2006). In the last two decades, increasing research effort has been devoted to moving towards more robust, integrated frameworks for separating and treating all sources of uncertainty (Liu and Gupta, 2007).

Beven and Binley (1992) introduced the generalized likelihood uncertainty estimation (GLUE) methodology for model calibration which assumes that the total uncertainty in the streamflow predictions can be characterized using solely model parameter uncertainty. However, uncertainties associated with input data and output data (i.e., data errors) are not explicitly considered. Thiemann et al. (2001) introduced the Bayesian recursive parameter estimation (BaRE) methodology that poses the parameter estimation problem within the context of a formal Bayesian framework. BaRE explicitly considers the uncertainties associated with model-parameter selection and output measurements, but input data uncertainty and model structural uncertainty are not specifically separated out and are only implicitly considered, by expanding the predictive uncertainty bounds in a somewhat subjective manner (Liu and Gupta, 2007). A variety of other frameworks that have moved the science forward in recent years include the Shuffled Complex Evolution Metropolis algorithm (SCEM) and extensions (Vrugt et al., 2003a,b), the DYNamic Identifiability Analysis framework (DYNIA) (Wagener et al., 2003), the maximum likelihood Bayesian averaging method (MLBMA) (Neuman, 2003), the dual state-parameter estimation methods (Moradkhani et al., 2005a,b), and the Simultaneous Optimization and Data assimilation algorithm (SODA) (Vrugt et al., 2005). However, these methods do not address all three critical aspects of uncertainty analysis (input error, structural error and output error) in a comprehensive, explicit and cohesive way (Liu and Gupta, 2007).

Despite the challenges in dealing with multiple sources of uncertainty, several important developments have taken place in the last decade. In particular, Kavetski et al. (2002, 2006a,b) introduced the Bayesian Total Error Analysis (BATEA) methodology, which explicitly characterizes input and output data uncertainty, and supports a stochastic description of structural errors (Kuczera et al., 2006), within a Bayesian framework. BATEA allows the modeller to specify error models for all sources of uncertainty and integrates these models into the posterior inference of model parameters and predictions. Similarly, Ajami et al. (2007) introduced the Integrated Bayesian Uncertainty Estimator (IBUNE), which combines a probabilistic parameter estimator algorithm and Bayesian model combination techniques to provide an integrated assessment of uncertainty propagation within a system. If successful, characterizing and separating individual sources of error would represent a significant advance in environmental uncertainty analysis.

In current applications of BATEA and IBUNE, input errors have been assumed to be multiplicative and independent: while both frameworks are model-independent, there has to date been little discussion of appropriate rainfall error models when using raingauge data to calibrate a hydrological model and subsequently use the model for forecasting. Other error models, such as *additive* Gaussian errors, have also been used (e.g., Huard and Mailhot, 2006). Radar rainfall applications traditionally assume additive Gaussian error where the variance depends (usually proportionally) on rainfall rate (Villarini and Krajewski, 2010). This results in an analogous distribution to the lognormal multiplicative error assumption often used in rainfall uncertainty studies within the hydrological community (e.g., Kavetski et al., 2006a; Renard et al., 2010); although with different skew characteristics.

Given the difficulties in understanding sampling errors in rainfall, almost all rainfall error models used in hydrology to date are highly conceptualized, e.g., hypothesizing multiplicative errors. More recent applications have begun to test some of the common assumptions, e.g., the data-driven sampling error model of Villarini and Krajewski (2008). In particular, Moulin et al. (2009) explore rainfall error model structure in detail, developing and calibrating an error model for hourly precipitation rates combining geostatistical tools based on kriging and an autoregressive model to account for temporal dependence of errors. Models with additional complexity to enable representation of spatial and temporal error characteristics will be necessary where multiple rainfall inputs are needed (for applications where high rainfall resolution is required or for large catchments; we return to the issue of catchment size in the Discussion section). In cases where weather radars are used to capture rainfall variability within a catchment, specialised error models can be used to generate ensembles of rainfall fields (e.g., Germann et al., 2009; Villarini et al., 2009; AghaKouchaka et al., 2010). Finally, in order to ensure statistical and computational well-posedness of the inference, typical applications apply the multiplicative assumption either to entire storm events (preserving the pattern but allowing for depth errors, Kavetski et al., 2006b), or to individual days with high leverage on model predictions (determined using sensitivity analysis, Thyer et al., 2009).

Fundamentally, progressive disaggregation of individual sources of uncertainty requires more detailed probabilistic models describing the uncertainty in each data source, increasing the complexity of the inference problem. Meaningful development and application of these hypotheses necessarily require reliable quantitative a priori information. In the absence of such knowledge, unsupported assumptions may be made, undermining the integrity of the inference. In particular, input error is likely to interact with model structural error, making posterior distributions of rainfall model-dependent, as well as affecting the inference of model parameters themselves (Beven, 2004; Kuczera et al., 2006; Balin et al., 2007; Thyer et al., 2009). It is critical that data error models should be developed using data analysis that is independent from the hydrological model calibration, to bring genuine independent information into the inference (Renard et al., 2010). This paper is a step in this direction, where we test the common multiplicative rainfall error model and comment on its suitability for use at varying temporal scales of the hydrological model.

4. Site and campaign description

The Mahurangi catchment is located in the North Island of New Zealand (Fig. 1a). The Mahurangi River drains 50 km^2 of steep hills and gently rolling lowlands; catchment elevations range from 250 m above sea level on the northern and southern boundaries, to near sea level at Warkworth on the east coast. Approximately half of the catchment (the central lowlands) is planted in pasture; one quarter of the catchment is in plantation forestry; and one quarter native forest. The catchment's soils have developed over Waitemata sandstones, which typically display alternating layers of sandstone and siltstone. Most soils in the catchment are clay loams, no more than a metre deep; clay and silt loam soils are also present in some parts of the catchment.

The climate is generally warm and humid, with mean annual rainfall of 1628 mm and mean annual pan evaporation of 1315 mm. Frosts are rare, and snow and ice are unknown. In late summer (February and March), remnants of tropical cyclones occasionally pass over northern New Zealand, producing intense bursts of rain. Convective activity is significant over the summer, whereas the majority of the winter rain comes from frontal systems. Maximum rainfall is usually in July (the middle of the austral winter), while maximum monthly temperature and pan evaporation occur in January or February.

The catchment was extensively instrumented during the period 1997–2001 (refer to Woods et al. (2001) for further details): data from 29 nested stream gauges and 13 raingauges was complemented by measurements of soil moisture, evaporation and tracer experiments. We describe here only the rainfall data collection. The location of the 13 raingauges is shown in Fig. 1b; rainfall depths were measured every 2 min using standard 200 mm collectors and 0.2 mm tipping buckets. The rainfall data was subject to manual quality control and data from malfunctioning gauges were removed from the analyses which follow. To augment the rainfall observations, the Physics Department of the University of Auckland deployed a mobile X-band radar for intensive campaigns of 1–2 month duration. This radar was sited in the southwest corner of the catchment and resolves rainfall on a 150 m grid, every 5 s (typically aggregated to 2-min average values), for the whole of the catchment. The rainfall radar estimates are processed and corrected for bias: for details refer to Nicol (2001) and Nicol and Austin (2003).

5. Analysis

Our investigation of the rainfall data available in the Mahurangi catchment is divided into two main themes.

The first part analyses the spatial variability and uncertainty in rainfall when considered solely as a binary (two-state) process. In other words, what is the consistency of wet and dry periods over the catchment? This type of analysis is a crucial check on the assumptions underlying multiplicative rainfall error models, since the latter cannot account for rain events with only partial catchment cover that are entirely missed by a raingauge. In this paper we focus only on the multiplicative error model used in previous

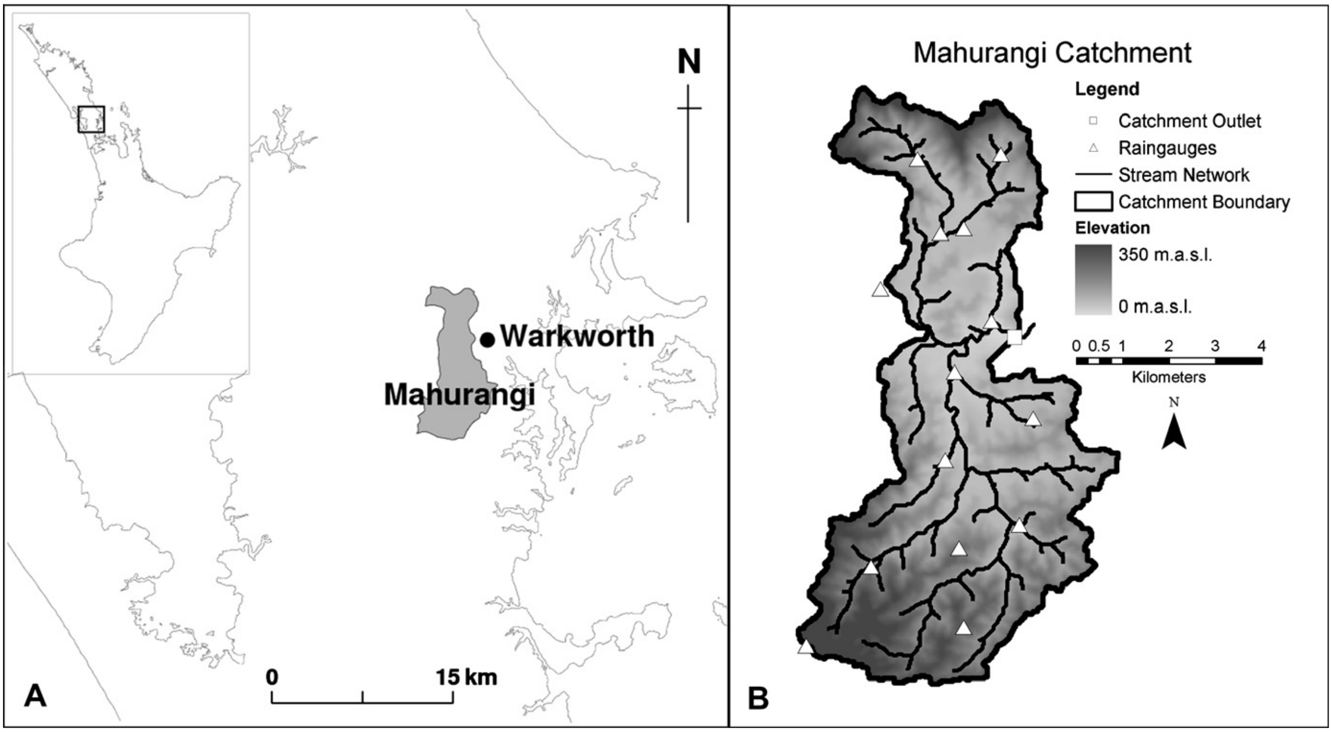

Fig. 1. (A) Mahurangi catchment location map. (B) Raingauge locations and stream network in the Mahurangi catchment.

research on directly incorporating rainfall uncertainty into hydrological calibration (e.g., Kavetski et al., 2002; Ajami et al., 2007). However we recognise that more complex approaches are also possible, for example by considering conditional probabilities for rainfall in each catchment 'pixel', based on the measured rainfall and modulated by spatially correlated random fields to signify the probability of a correct measurement. This method has been demonstrated in the context of both station data (Clark and Slater, 2006) and remote sensing-based rainfall fields (Hossain and Anagnostou, 2006; Hossain, 2007; Germann et al., 2009; Villarini et al., 2009; AghaKouchaka et al., 2010).

The second part examines the consistency of rainfall quantities over the catchment; based both on complete rainfall records and also for individual storm events when correct estimation of rainfall is most crucial. This allows us to estimate the statistical distributions of rainfall multipliers and test if these could form the basis of an adequate rainfall error model. In addition, analysis of rainfall profiles at a given gauge during individual storm events is used to put multipliers into the context of an event and understand interactions between temporal and spatial variability within a storm.

5.1. Rainfall state

5.1.1. Raingauges

Records from the 13 raingauges in the Mahurangi catchment are available as a complete series from 1997 to 2001. Although some of the records are available at shorter timesteps, all are aggregated to 15 min intervals: typical of the timestep used in a high-resolution hydrological model and designed to be sufficiently long to reduce the influence of random instrument/sampling errors which might otherwise be difficult to distinguish from true spatial variation in rainfall. The analyses are also repeated with rainfall aggregated to 1 h measurements, in order to understand changes in rainfall variability (and hence suitable error formulations) as a function of the temporal data resolution.

Our initial hypothesis was that the consistency of rainfall over the catchment is related to the severity of the storm event; i.e., that drizzle or low intensity rainfall might be patchy across the catchment but that heavy rainfall was more likely to be part of an extended weather system covering the complete catchment. A possible exception might be convective rainfall which could produce intense but localised showers.

To test this hypothesis, rainfall at each timestep over a 4.1 year period (28/07/1997–11/09/2001) was tallied according to mean rainfall intensity (taken over all gauges in the catchment) and number of gauges recording rainfall. These results are plotted in Fig. 2 below. The analysis shows that, using the hourly data (Fig. 2A), where mean rainfall intensity recorded by the gauges is greater than 1 mm/h, rainfall occurs in at least (any) 12 of the 13 gauges at least 94% of the time. Rainfall coverage values are given as equivalent number of gauges assuming all are functional, however the analysis was performed using percent coverage values to allow for gauge data removed during quality control. For intensities 1 mm/h or greater, the consistency of rainfall across the catchment therefore suggests that a multiplicative error model for rainfall would be suitable regardless of the location of the raingauge in the catchment. Note that rainfall intensities higher than those shown in Fig. 2 were recorded in the catchment: the plot shows only cases where some gauges were not recording rainfall. Comparing the CDF plots for 15-min data and hourly data, it can be seen that variability in wet/dry states across the catchment becomes more pronounced at shorter time scales. For example, at rainfall intensities greater than 1 mm/h, rainfall is only captured at 12 or 13 gauges 70% of the time. The threshold for suitability of the multiplicative error model is therefore time-scale dependent. The choice of threshold is also clearly dependent on the required level of accuracy: at intensities over 1.5 mm/h only 81% capture at 12 or more gauges is obtained, by 2 mm/h capture reaches 86% and 90% capture does not occur until intensities exceed 2.6 mm/h.

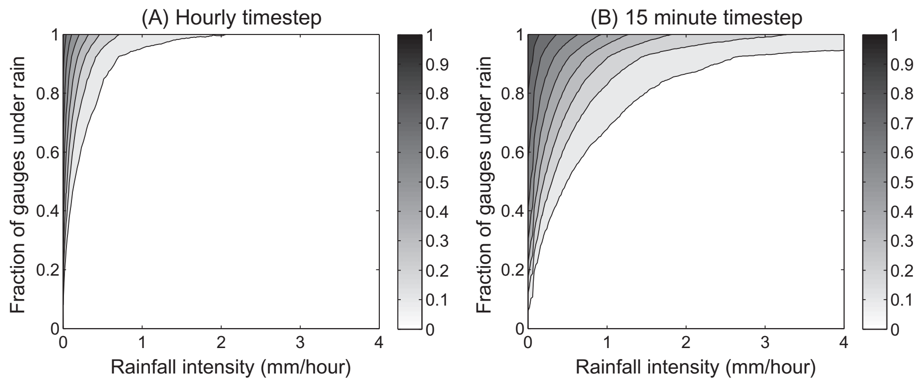

Fig. 2. Consistency of rainfall state across raingauges for different threshold rainfall intensities, at (A) hourly and (B) 15-min timesteps.

5.1.2. Radar

Radar data provides much more detail about the spatial variation in rainfall state (wet/dry) as it is resolved on a 150 m grid. The availability of this extremely high-resolution (spatial and temporal) radar provides an excellent and unusual opportunity to examine consistency of rainfall across the catchment and hence identify appropriate thresholds for multiplicative error model use. However, radar data is only available for specific field campaign periods (approximately 28 days total during the 4-year rainfall measurement period), and hence the data are used to provide supplementary evidence to compare with conclusions drawn from the raingauge data analysis. The time periods used for this investigation were the five storm events captured with the radar, as follows: 7/8/98–12/8/98, 26/8/98–28/8/98, 15/9/98–18/9/98, 3/11/99–4/11/99, 9/11/99–13/11/99. Rainfall intensities measured by the radar were aggregated to timesteps of 15 min, 1 h and 24 h, for comparison.

As with the raingauge data, the first analysis was intended to investigate the consistency of rainfall estimates over the catchment. Spatial consistency in the rainfall fields can be quantified more exactly using radar data than with raingauges, expressed here as the proportion of the catchment under rainfall. Fig. 3 below shows simple histograms of this proportion, for the three different timesteps of aggregation.

As before, we also quantify the relationship between mean intensity of rainfall and consistency of rainfall, by plotting average catchment rainfall against fraction of catchment under rainfall, using the radar data (Fig. 4A). For comparison, the figure also shows the raingauge data over the time periods where the radar was operational (Fig. 4B).

The results show that, using radar data at a 15 min timestep (Fig. 4A2), there are a significant number of periods during storm events where rainfall is scattered over the catchment (for 35% of timesteps, between 10% and 90% of the catchment is under rainfall). As expected, at an hourly timestep (Fig. 4A1), rainfall appears more uniform in time (42% of timesteps with less than 10% rainfall, 31% of timesteps between 10% and 90% rainfall and 27% of timesteps with greater than 90% rainfall). Finally, at a daily timestep, it was unusual to find significant dry areas of the catchment during a storm day (Fig. 3).

The cumulative plots of fraction of catchment under rainfall against intensity (Fig. 4A) shows reasonable consistency with the corresponding results using the gauge network (Fig. 4B for restricted time period and Fig. 2 for full record). The analysis using the restricted raingauge record shows some differences, especially at an hourly timestep when even at high rainfall thresholds there is often one gauge not recording rain. In part these differences are likely to be due to the small number of data points available (both number of gauges and timesteps). However, in general, it is reassuring that the thresholds for the suitability of the multiplicative error model appear similar when derived from radar vs. from raingauge data: 1 mm/h for hourly data (Figs. 2A and 4A1) and 2–3 mm/h for 15 min data (Figs. 2B and 4B2). For a daily timestep, an intensity criterion would not be necessary (not shown). The similarity of the results using the gauge network and radar data suggests that the threshold values are reliable and not an artefact of the sampling scheme, e.g., the number and/or configuration of raingauges.

We therefore conclude that a multiplicative error model is consistent with observed rainfall spatial variability in the Mahurangi catchment, and is suitable for use in hydrological modelling in this location, where an appropriate minimum rainfall intensity threshold is respected. On the assumption that analogous error structures arise in other catchments, the results support the suitability of the approach taken in current applications of the BATEA model calibration strategy (Thyer et al., 2009), where rainfall multipliers are

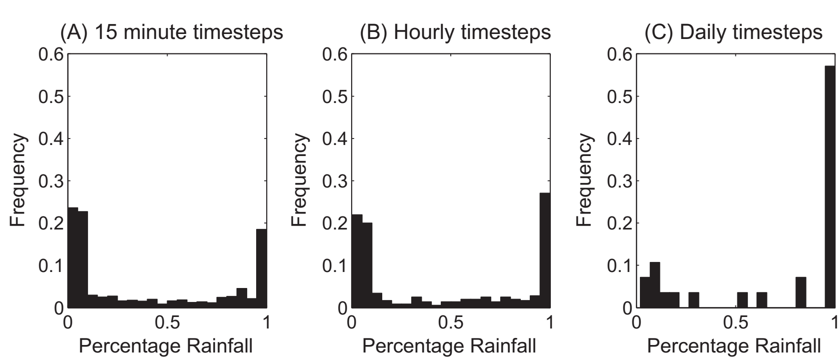

Fig. 3. Distributions of catchment area under rainfall at different timesteps, for five storm events.

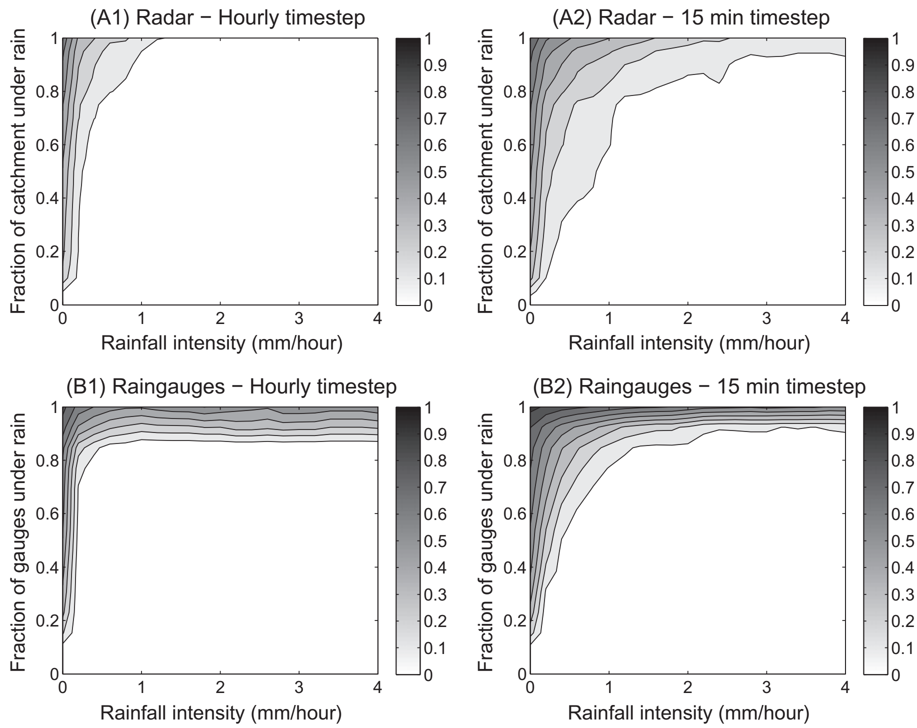

Fig. 4. Consistency of rainfall state across radar pixels for different critical rainfall intensities, at (A1) hourly and (A2) 15-min timesteps, and across raingauges for identical time periods (B1) hourly and (B2) 15-min timesteps.

applied only to days where the model is sensitive to rainfall uncertainty (estimated using a priori sensitivity analysis), which generally correspond to high-rainfall days. Future studies would be valuable to investigate the transferability of these results to other regions characterized by different rainfall regimes, and different catchment sizes.

5.2. Rainfall quantity

5.2.1. Distributions of rainfall totals

Where rainfall occurrence is consistent across the catchment and hence suitable for representation by a multiplicative error model, the distribution (type and parameters) of multipliers must be specified. Previous studies have in general specified multipliers as arising from a lognormal distribution with zero mean (Kavetski et al., 2006a,b), or unknown mean (Thyer et al., 2009). The data at Mahurangi allows us to directly test this hypothesis.

In order to calculate the error multiplier at a given timestep, the true areal mean rainfall must be estimated. The multi-gauge sample mean is typically used as a proxy for the value. Previous authors have investigated the uncertainty in this estimate, which is highly dependent on the raingauge network configuration in relationship to rainfall spatial covariance. Estimation procedures have been developed for long-term areal means for specific network configurations (Rodríguez-Iturbe and Mejía, 1974) and in the general case (Morrissey et al., 1995); and for instantaneous areal means in the context of use of raingauge data to calibrate rainfall radar (Ciach and Krajewski, 1999; Villarini et al., 2008). Where the contribution of small-scale variability and measurement error is significant, the benefit of clusters of raingauges (i.e., within a distance of a few metres) has also been emphasised (Bradley et al., 2002; Ciach and Krajewski, 1999; Mandapaka et al., 2009; Villarini et al., 2008; Young et al., 1999).

In this study, we used the multi-gauge sample mean to estimate the areal mean. In the Mahurangi catchment, the dense raingauge network (13 gauges within a 50 km^2 area) makes this a reasonable estimate, and the quasi-uniform distribution of gauges by location and elevation within the catchment minimises the uncertainty given the number of gauges (Morrissey et al., 1995). The consistency in rainfall profiles between raingauges (discussed in Section 5.2; Fig. 9) provides further evidence that the raingauge density is sufficient in relation to the climatic conditions which control rainfall variability in the catchment. However, for the purposes of calculating the error multiplier, it is the relative magnitude of uncertainty in the estimate of the mean, in comparison to the variation of individual gauges around the mean, that is of more importance than the absolute uncertainty. Given the fixed sample size of 13 gauges (or infrequently, fewer due to data points removed during quality control), this is acknowledged as a limitation of the study which introduces uncertainty into the estimation of rainfall multipliers. The uncertainty is also dependent on the time scale of the analysis and on the characteristic correlation time of the rainfall process. The spatial uncertainty could only be reduced by using a denser gauge network in relationship to the rainfall spatial covariance structure; i.e., to increase the number of gauges without increasing the 'variance reduction factor' described by Rodríguez-Iturbe and Mejía (1974). However the same authors show experimentally that the reduction in uncertainty from adding a new gauge rapidly decreases as the number of existing gauges increases.

For each of the 13 raingauges, and for each storm timestep (defined as mean catchment rainfall greater than 0.2 mm/h and at least six gauges recording rainfall), the corrective multiplier was calculated in order to transform rainfall measured at the gauge into the estimated areal mean rainfall over the 13 gauges. These distributions are plotted in Fig. 5 below, for both 15 min and hourly timesteps, along with the mean and standard deviation of the empirical multiplier distribution, and the unbiased (zero) line for comparison. An additional plot is shown with all distributions overlaid for comparison.

Following the same methodology as for the raingauges, the radar data analysis was repeated using the 28 days, at both 15 min and hourly timescales. Gauged records were approximated using

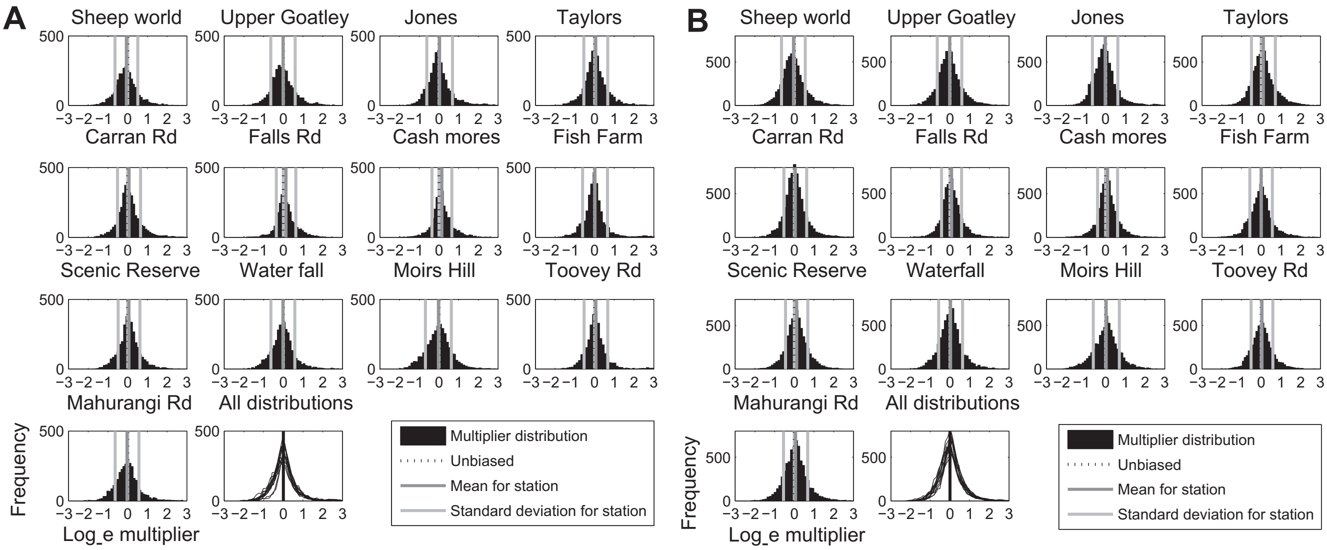

Fig. 5. Multipliers (log value) required to convert raingauge readings to catchment mean rainfall at (A) hourly and (B) 15-min timesteps.

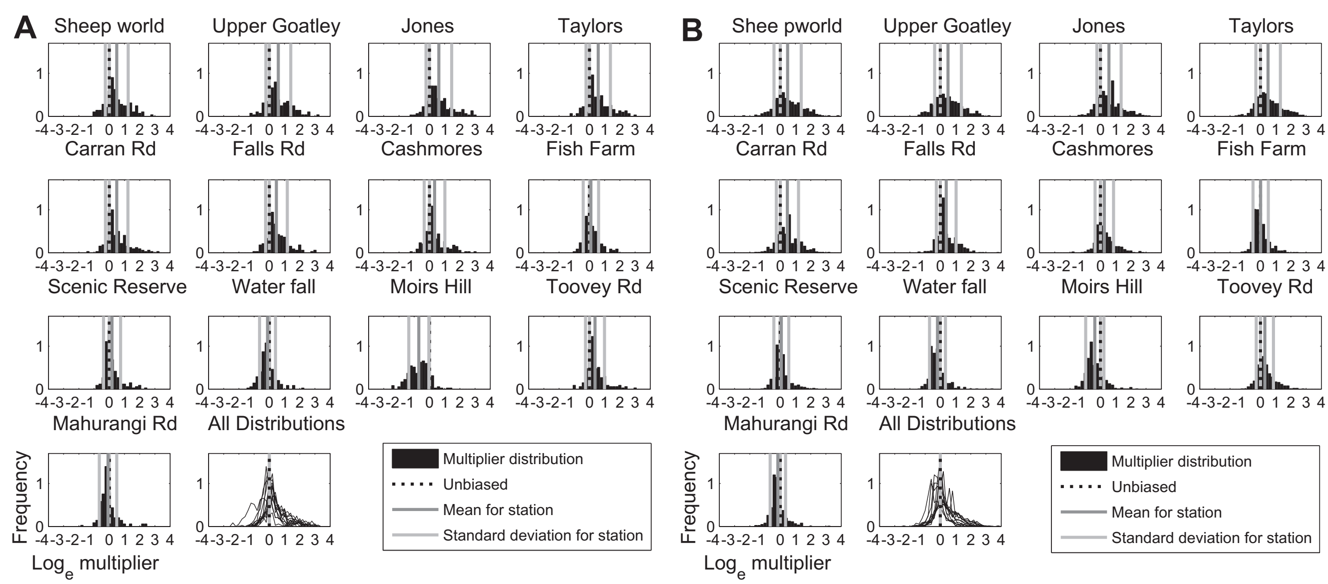

Fig. 6. Multipliers (log value) required to convert radar readings at raingauge locations to catchment mean rainfall measured by radar, at (A) hourly and (B) 15-min timesteps.

the radar pixel closest to the gauge location, and multipliers were calculated to transform this value to the catchment mean calculated from the complete radar data set (not just gauge locations). Results are shown in Fig. 6A and B.

The log multiplier distributions were tested for normality using the Lilliefors test, which is a modification of the Kolmogorov–Smirnov test for use where the mean and variance of the distribution to be tested have been estimated from the data (as is common in climate applications (Steinskog et al., 2007)). The log-normality hypothesis was rejected for all 13 sites using the raingauge data, and for 12 of the 13 sites using the radar data (the exception being Upper Goatley).

The distributions of the log-multipliers calculated using both 15-min data and hourly data were summarised using quantile–quantile plots (Fig. 7). Distributions are shown for raingauge log-multipliers, radar log-multipliers, and raingauge log-multipliers restricted to time periods when radar was available, for comparison. The QQ-plots show the excess kurtosis causing rejection of the log-normality hypothesis,(Fig. 7-1) as a lognormal distribution does not fully capture the positive tail of the empirical multiplier distribution. Quantile–quantile plots are also used to compare the log multiplier distributions to the logistic distribution (Fig. 7-2) and Laplace distribution (Fig. 7-3), which have higher excess kurtosis values of 6/5 and 3 respectively (compared to 0 for the Gaussian fit to log-multipliers). Using the Lilliefors test (as previously described) the quality of the fit is shown to be slightly improved for the (log-)Laplace over the lognormal and (log-)logistic distributions. For example, for the raingauge data at hourly timescale, the Laplace is accepted at two sites out of 13 at a 5% significance level, whereas the logistic and lognormal are rejected at all sites. The figures provide more information, showing that a trade-off occurs between the fit of the negative and positive tails of the distribution, as the kurtosis of the fitting distribution increases. To improve the fit to both tails simultaneously, either

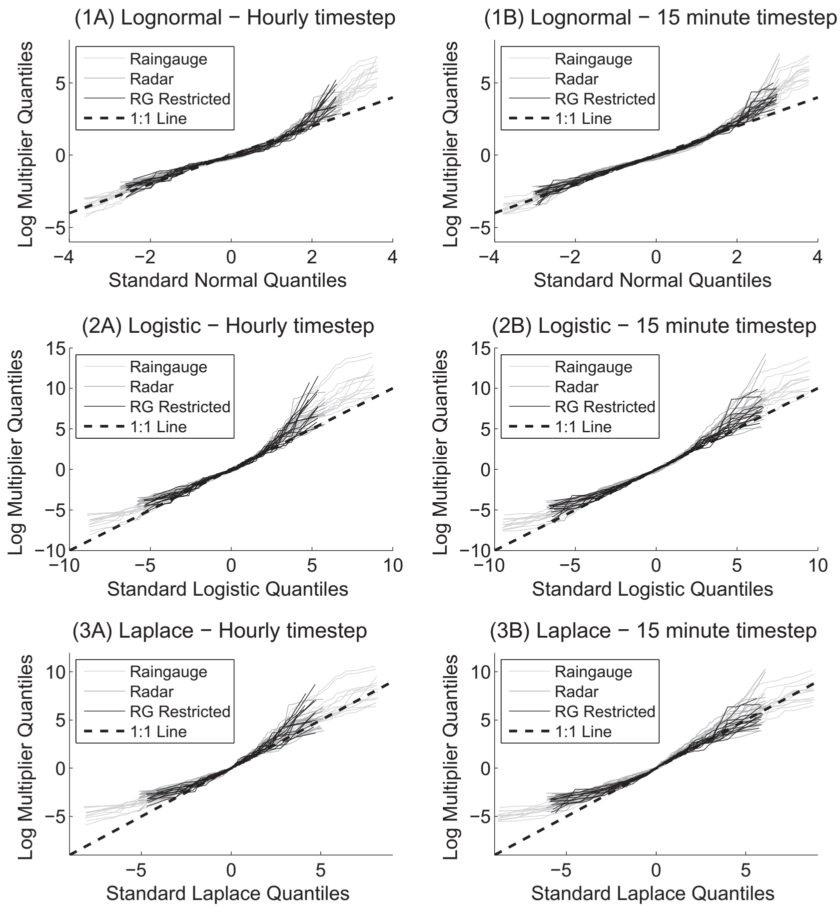

Fig. 7. QQ-plot of log multiplier distribution against (1) normal, (2) logistic, and (3) Laplace distributions for raingauge and radar data at (A) hourly and (B) 15-min timestep.

a non-symmetric distribution or alternatives to the log transform could be considered in future work (and judged against the likely increase in the number of fitted parameters).

When multiplicative error models for rainfall are used in hydrological modelling applications, the assumptions are typically made that rainfall multipliers are uncorrelated in time and have an invariant distribution (Kavetski et al., 2006a,b). Autocorrelations of the empirical multiplier series were calculated: at an hourly timestep the maximum autocorrelation occurs at lag 1, with a mean value of 0.15 over all gauges, and decreases rapidly for higher lags. At a 15-min timestep the value is increased to 0.34. Therefore for models operating at a 15-min timestep where multipliers are applied to consecutive timesteps, an autocorrelated error model may be warranted; however for models at an hourly timestep or where multipliers are applied only to selected heavy-rainfall timesteps, autocorrelation would be less important. Further studies are recommended to examine the transferability of these conclusions to regions with different rainfall regimes and/or different catchment sizes. More generally, in a method such as BATEA where individual error models are specified for each source of uncertainty, autocorrelation can be accounted for directly in the joint hyperdistribution of rainfall errors. In particular, the term $p(\phi|\beta_x)$ in Eq. (8) of Kavetski et al. (2006a), which to date has been used to represent independently distributed latent variables (multipliers) ϕ given hyper-parameters β_x, can readily accommodate correlated cases.

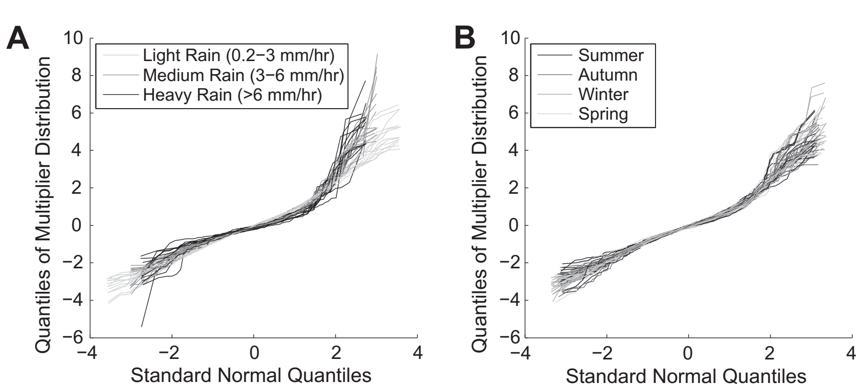

Fig. 8. QQ-plot of multiplier distribution quantiles against normal distribution quantiles, for raingauge data at hourly timestep, compared by (A) rainfall depth and (B) season.

To test for invariance in multiplier distribution, comparisons were made amongst storm timesteps of different rainfall depth (Fig. 8A) and according to the season during which the rain fell (Fig. 8B). The figures show that the multiplier distribution does not vary significantly with season, although there is slightly more variation between gauges during the wetter seasons (winter and spring) than in the drier seasons (summer and autumn). The depth of rainfall does however affect the multiplier distribution: during light rain the distribution is closer to lognormal, even though the quality of the fit is poor; during heavy rainfall multipliers have increased skew and the distribution has heavier tails with more outliers. Although it is not unexpected that heavy rain events show more variation over the catchment (e.g., during convective rain), it should be noted that this variation may cause greater uncertainty in the areal mean rainfall estimated from the gauges, and hence greater errors in the multiplier values. Despite this, the result suggests that high multiplier values are associated with heavy rainfall and hence with true variation in rainfall processes, rather than with noise obscuring the signal at low rainfall depths. More generally, any identified non-stationarities in the distribution of rainfall errors can again be accommodated in the BATEA hyper-distribution term (e.g., using covariates such as rainfall magnitude, season, and storm type).

5.2.2. Raingauge vs. radar data

Fig. 7 permits comparisons between multipliers derived using raingauge data (improved temporal coverage; reduced spatial coverage), radar data (shorter temporal coverage, improved spatial coverage), and restricted raingauge data (shorter temporal coverage, reduced spatial coverage). Consider first differences in temporal coverage between raingauge multipliers, and radar/restricted raingauge multipliers. Reduced temporal coverage gives rise to a more pronounced skew in the distributions, especially at 15-min timescale. In addition, the restricted data show noticeable changes in error distribution between gauges, unlike the full raingauge dataset, where the errors tended to follow a more consistent shape. Application of the two-sample Kolmogorov–Smirnov test leads us to reject the hypothesis that raingauge multipliers from full vs. restricted temporal coverage come from the same distribution in eight out of 13 sites (hourly timestep) and 10 out of 13 sites (15 min timestep).

An important distinction is that the radar data (and hence also the restricted raingauge data) covers predominantly storm periods, and multiplier distributions are more skewed during large storms (Fig. 8A). For example, if only timesteps where the raingauge reading is greater than 2 mm per 15 min are considered, skewness typically triples (although this effect may be partly due to the resulting change in sample size). The result is particularly pronounced in atypical areas of the catchment, such as Moirs Hill, which lies in the hills in the South-West of the catchment and consistently records higher than average rainfall in response to orographic rainfall effects. Increased skewness during storm events must be accounted for if rainfall multipliers are to be applied to high-rainfall days only (as in the BATEA case study of Thyer et al., 2009), and suggests that a skewed distribution together with careful siting of the raingauge would be necessary to capture the multiplier distribution even in a relatively small basin such as the Mahurangi.

Second, consider differences in spatial coverage between multipliers calculated from radar vs. restricted raingauge data. Despite visual similarity between the multiplier distributions, two-sample Kolmogorov–Smirnov tests reject the hypothesis that these data originate from the same distribution in 11 out of 13 sites (at hourly timestep) and all sites (15 min timestep). It is likely that the more complete sampling of catchment rainfall provided by the radar, including the more inaccessible hillcountry and bush areas where raingauges are more difficult to site, is in part responsible for these differences. However, the susceptibility of radar data to transient errors from sources such as changes in the rainfall field between the measurement height and the ground, and recording the reflectivity data with a limited radiometric resolution may also play a role (e.g., Fabry et al., 1994; Nicol and Austin, 2003; Jordan et al., 2000; Villarini and Krajewski, 2010).

It is also interesting to note the differences in the representativeness of individual gauges. For example, the Toovey Road gauge is highly representative of the catchment mean rainfall, showing a strongly peaked distribution with mean close to zero, while other sites such as Falls Road are less representative for both raingauge and radar analyses. This observation echoes previous studies into representative areas of a catchment for given variables such as soil moisture, designed to reduce gauging requirements (e.g., Grayson and Western, 1998; Martinez-Fernandez and Ceballos, 2005; Vachaud et al., 1985).

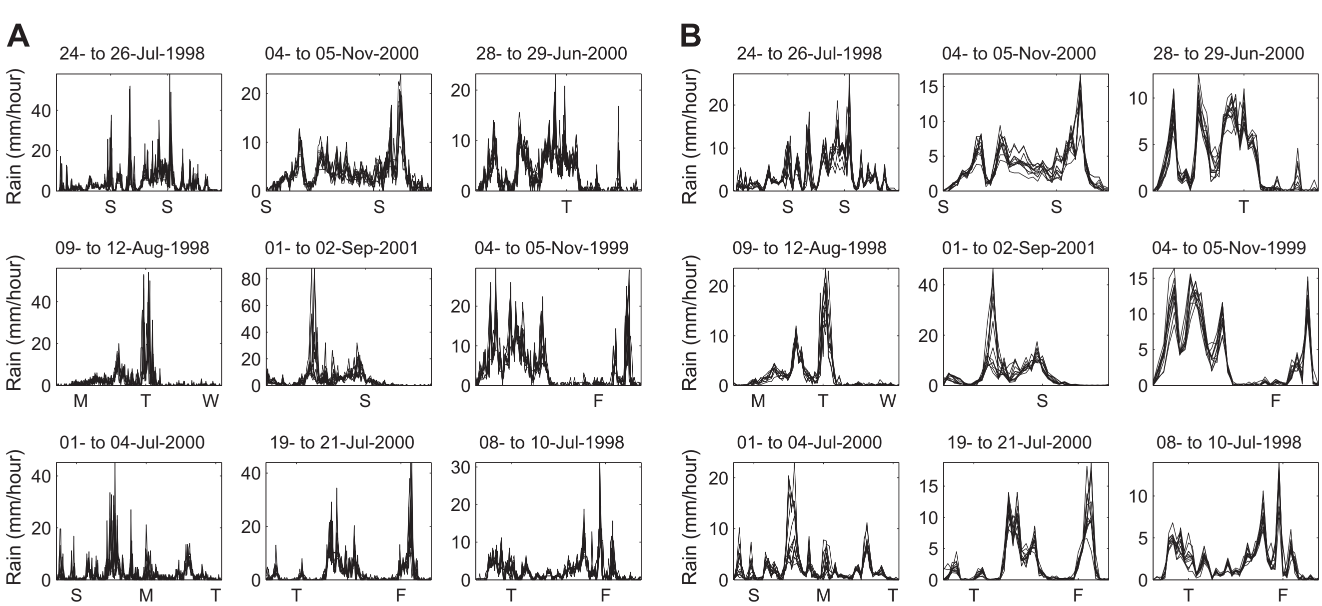

Fig. 9. Comparison of storm profiles at different raingauges, at (A) 15-min and (B) hourly timesteps.

5.2.3. Consistency in rainfall profiles

In view of the differences between raingauge and radar data, highlighted in the previous section, further investigation was carried out into the spatial and temporal variation in rainfall volumes. In particular, this analysis may provide insights into the increased variability in multiplier distributions in the radar data, not seen in the raingauge totals.

Firstly, spatial variation in rainfall totals was investigated. Hourly and 15-min rainfall profiles were extracted for all raingauges, for the nine largest storms over the study period (Fig. 9A and B).

Fig. 9 shows remarkably little variation in storm profile between raingauges, with peaks generally occurring at all gauges within a timespan of 1 h. This result may be due to an underlying lack of variability in rainfall or may rather be caused by the averaging effect of recording raingauge totals at hourly intervals, which could hide rainfall variability at short temporal scales. One storm where both 2 min and 15 min data are available from the radar is investigated in more detail: Fig. 10A below shows the storm profile at both 2 min and 15 min timesteps, for three of the raingauge locations. In addition, the multipliers from each of those gauges to the mean catchment rainfall are calculated, again at both 2 min and 15 min timesteps, and shown in Fig. 10B.

Secondly, the ability to capure peak rainfalls was examined. The peaks of rainfall intensity are significantly damped (Fig. 10A; max intensity reduced by more than 60% for some peaks) and this effect would lead to important changes in the tails of the multiplier distributions. Multiplier distributions are therefore time-scale dependent. The fluctuations caused by rain cells tracking over the catchment occur in the 2 min data, but much of the variation is lost in the 15 min data. The time for a typical rain cell to travel across the Mahurangi catchment has been estimated as close to 15 min, assuming raincell size of 1–5 km, a speed of the order of 10 m s^{-1} and a catchment width of 5–10 km (Woods et al., 2001). We conclude that in this case, consistency between raingauges at 15 min is due mainly to the averaging effect seen at timescales longer than the time taken for a raincell to traverse the catchment. When using spatial maps of radar data to calculate multipliers, as oppose to raingauges, more of this variation may be captured as areas both directly under the track of the raincell, and those on the edge of the rain area, are fully sampled.

6. Discussion and conclusions

Our investigation of rainfall variability within the dense gauge/radar network at Mahurangi has highlighted some important results for understanding rainfall uncertainty and deriving data-based probabilistic error models for use in hydrological calibration.

Our examination of the variability of wet/dry states over the catchment has confirmed that multiplicative error is a suitable formulation for correcting mean catchment rainfall values during high-rainfall periods (e.g., intensities over 1 mm/h); or for longer timesteps at any rainfall intensity (timestep 1 day or greater). We suggest that the effect of timestep on multiplier suitability is regulated by catchment size: specifically the time required for typical raincells to cross the catchment could be used as a first estimate of critical timestep.

We found that the standard distribution used for rainfall multipliers, the lognormal, provides a reasonable fit to the negative tail of the empirical multiplier distributions, but fails to capture the greater excess kurtosis and skew in the positive tail. Therefore, alternative distributions should be considered, especially since the tails of the multiplier distribution represent large rainfall errors and may significantly impact on streamflow model predictions. The logistic and Laplace distributions, which have higher excess kurtosis values of 6/5 and 3 respectively, were also tested. Although these heavier-tailed distributions improve the fit to the positive tail, an asymmetric distribution would be required to reproduce the skew in the observed error distribution. This would be most important during heavy rainfall events which were shown to have notably higher skews in the multiplicative errors. It was also found that, in the Mahurangi catchment, the error distributions do not vary significantly with season and hence a time-invariant distribution is sufficient.

More broadly, our results suggest that more sophisticated error models than the standard lognormal hypothesis may be justified in hydrological model calibration, prediction and uncertainty studies using rainfall–runoff models. Bayesian methods such as BATEA are entirely general with respect to the error model used – they can accommodate daily – or storm-wise multipliers (Thyer et al., 2009), autocorrelation, and seasonality, provided these are supported by independent data analysis. In view of the interactions

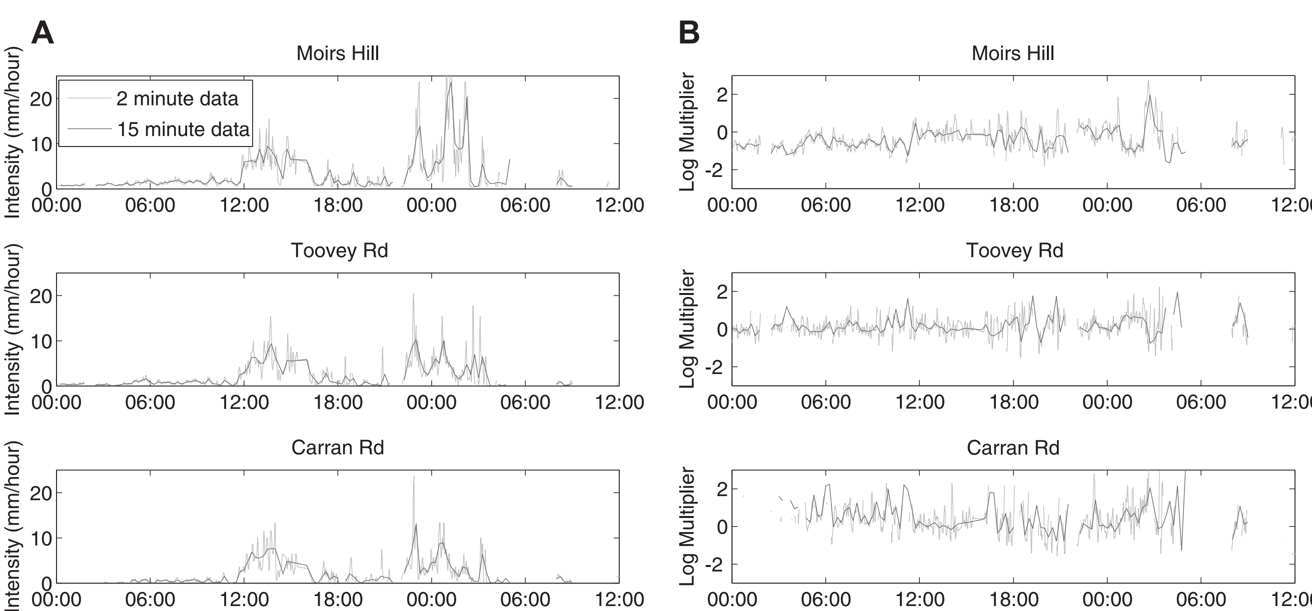

Fig. 10. Comparison of (A) storm profiles and (B) log-multipliers, calculated at 2 min and 15-min timesteps for the rainstorm of 10–11 August, 1998, for three raingauge sites.

between the different sources of error shown quantitatively by Renard et al. (2010), we stress that the derivation of data error models should exploit any independent insights to the maximum extent possible, to provide the best opportunity to improve the predictive ability of the inferred hydrological models.

An important question to ask is how the results and conclusions might be extended to other catchments of different sizes, climates and rainfall patterns/consistencies. For example, in larger catchments, partial storm coverage might be more common even when rainfall event totals are considered. As previously stated, our findings suggest that the general suitability of a multiplicative error model can be assessed by comparing the dimensions of the catchment area that any raingauge is expected to represent, with the distance travelled by a typical raincell over a given timestep. The prevailing direction of storm movement would hence also be an important factor in this assessment.

We also considered the relationship between results from a raingauge network vs. a high-resolution rainfall radar. The two measurement types indicated consistent rain rate thresholds above which a multiplicative error formulation was appropriate. Therefore in other catchments where a similar analysis is conducted, but high-resolution radar is not available, we suggest that the use of a raingauge network would give reliable guidance on threshold estimates. In terms of the shape of the multiplier distribution, Kolmogorov–Smirnoff tests discriminated between the distributions derived from the raingauge network vs. radar, although QQ-plots (Fig. 7) showed that the distributions were visually similar. We therefore suggest that a dense raingauge network may provide a working estimate of the multiplier distributional form, but should not be relied upon to fully capture the shape of this distribution.

The dense monitoring network at Mahurangi draws our attention to the time/space complexity of rainfall behaviour that cannot be corrected by a simple multiplicative error on measured rainfall. Intense bursts of rainfall occur at short space or time scales (refer to the long tails of the multiplier distributions (Figs. 5 and 6) and increased variability in multipliers at the 2 min timescale (Fig. 10)) which would not be apparent when using catchment average data at typical model timescales. This additional knowledge has the potential not only to inform statistical models of rainfall uncertainty, but also to change our understanding of the catchment processes and hence our conceptual model of the catchment. A range of 'fast-response' processes such as infiltration excess flow, transient overland flow or macropore flow would be under-represented in models where catchment average rainfall is used; or cause compensatory effects in model calibration to correct the bias. Additional mechanisms (e.g., a distribution function approach to rainfall input; see Liang et al. (1996) for an example) would be required in a hydrological model that aims to capture the full effects of rainfall variability.

While this study focuses on a single catchment, follow-up studies on different catchments are clearly needed to continue improving our understanding of rainfall error characteristics and their relationship to catchment size, topography and climate. A comparison of the suitability of different error models could be made in several catchments with dense raingauge networks and/or rainfall radar such as Walnut Gulch (Moran et al., 2008) or Sabino Canyon in Arizona (Lyon et al., 2008); or the Brue catchment in England (Villarini and Krajewski, 2008).

Acknowledgements

Financial support for this project was provided by the New Zealand Foundation for Research Science and Technology Grant CO1X0812. The authors wish to thank all participants of the MARVEX campaign and particularly Prof. Geoff Austin of the University of Auckland for use of the X-band radar data. The authors would also like to acknowledge review comments from Hoshin Gupta and an anonymous reviewer, which significantly contributed to the improvement of the manuscript.

References

AghaKouchaka, A., Bardossy, A., Habib, E., 2010. Conditional simulation of remotely sensed rainfall data using a non-Gaussian v-transformed copula. Adv. Water Resour. 33 (6), 624–634.

Ajami, N.K., Duan, Q., Sorooshian, S., 2007. An integrated hydrologic Bayesian multimodel combination framework: confronting input, parameter and model structural uncertainty in hydrologic prediction. Water Resour. Res. 43, W01403,2. doi:10.1029/2005WR004745.

Astin, I., 1997. A survey of studies into errors in large scale space–time averages of rainfall, cloud cover, sea surface processes and the earth's radiation budget as derived from low earth orbit satellite instruments because of their incomplete temporal and spatial coverage. Surv. Geophys. 18, 385–403.

Balin, D, Shbaita, H., Lee, H., Rode, M., 2007. Extended Bayesian uncertainty analysis for distributed rainfall–runoff modelling: application to a small lower mountain range catchment in central Germany. In: Proc CAIWA Conference on "Coping with Complexity and Uncertainty", Basel, Switzerland, November, 2007.

Bárdossy, A., Das, T., 2008. Influence of rainfall observation network on model calibration and application. Hydrol. Earth Syst. Sci. 12, 77–89.

Bell, T.L., Kundu, P.K., 2000. Dependence of satellite sampling error on monthly averaged rain rates: comparison of simple models and recent studies. J. Climate 13, 449–462.

Beven, K., 2004. Rainfall–Runoff Modelling – The Primer. John Wiley & Sons Ltd., New York.

Beven, K., Binley, A.M., 1992. The future of distributed models: model calibration and uncertainty prediction. Hydrol. Processes 6, 279–298.

Borga, M., 2002. Accuracy of radar rainfall estimates for streamflow simulation. J. Hydrol. 267 (1–2), 26–39.

Bradley, A.A., Peters-Lidard, C., Nelson, B.R., Smith, J.A., Young, C.B., 2002. Raingage network design using NEXRAD precipitation estimates. J. Am. Water Resour. Assoc. 38, 1393–1407.

Bras, R.L., Rodriguez-Iturbe, I., 1976. Network design for the estimation of the areal means of rainfall events. Water Resour. Res. 12, 1185–1195.

Carpenter, T.M., Georgakakos, K.P., 2004. Impacts of parametric and radar rainfall uncertainty on the ensemble streamflow simulations of a distributed hydrologic model. J. Hydrol. 298 (1–4), 202–221.

Chapon, B., Delrieu, G., Gosset, M., Boudevillain, B., 2008. Variability of rain drop size distribution and its effect on the Z–R relationship: a case study for intense Mediterranean rainfall. Atmos. Res. 87, 52–65.

Ciach, G.J., 2003. Local random errors in tipping-bucket rain gauge measurements. J. Atmos. Oceanic Technol. 20, 752–759.

Ciach, G.J., Krajewski, W.F., 1999. On the estimation of radar rainfall error variance. Adv. Water Resour. 22, 585–595.

Clark, M.P., Slater, A.G., 2006. Probabilistic quantitative precipitation estimation in complex terrain. J. Hydrometeorol. 7 (1), 3–22.

Crow, W.T., Van Loon, E., 2006. Impact of incorrect model error assumptions on the sequential assimilation of remotely sensed surface soil moisture. J. Hydrometeorol. 7 (3), 421–432.

Fabry, F., Bellon, A., Ducan, M.R., Austin, G.L., 1994. High-resolution rainfall measurements by radar for very small basins – the sampling problem reexamined. J. Hydrol. 161, 415–428.

Gebremichael, M., Krajewski, W.F., 2004. Characterization of the temporal sampling error in space–time-averaged rainfall estimates from satellites. J. Geophys. Res. – Atmos. 109.

Gebremichael, M., Krajewski, W.F., 2005. Effect of temporal sampling on inferred rainfall spatial statistics. J. Appl. Meteorol. 44, 1626–1633.

Germann, U., Berenguer, M., Sempere-Torres, D., Zappa, M., 2009. REAL-ensemble radar precipitation estimation for hydrology in a mountainous region. Quart. J. Roy. Meteorol. Soc. 135, 445–456.

Gotzinger, J., Bardossy, A., 2008. Generic error model for calibration and uncertainty estimation of hydrological models. Water Resour. Res. 44.

Grayson, R.B., Western, A.W., 1998. Towards areal estimation of soil water content from point measurements: time and space stability of mean response. J. Hydrol. 207, 68–82.

Habib, E., Krajewski, W.F., Kruger, A., 2001. Sampling errors of fine resolution tipping-bucket rain gauge measurements. J. Hydrol. Eng. 6 (2), 159–166.

Hossain, F., 2007. A two-dimensional satellite rainfall error model. IEEE Trans. Geosci. Remote Sens. 45, 275 (vol. 44, p. 1511, 2006).

Hossain, F., Anagnostou, E.N., 2005a. Numerical investigation of the impact of uncertainties in satellite rainfall and land surface parameters on simulation of soil moisture. Adv. Water Res. 28 (12), 1336–1350.

Hossain, F., Anagnostou, E.N., 2005b. Using a multi-dimensional satellite rainfall error model to characterize uncertainty in soil moisture fields simulated by an offline land surface model. Geophys. Res. Lett. 32, L15402. doi:10.1029/2005GL023122.

Hossain, F., Anagnostou, E.N., 2006. Assessment of a multidimensional satellite rainfall error model for ensemble generation of satellite rainfall data. IEEE Geosci. Remote Sens. Lett. 3, 419–423.

Hossain, F., Huffman, G.J., 2008. Investigating error metrics for satellite rainfall at hydrologically relevant scales. J. Hydrometeorol. 9 (3), 563–575.
Huard, D., Mailhot, A., 2006. A Bayesian perspective on input uncertainty in model calibration: application to hydrological model /u201cabc/u201d. Water Resour. Res. 42. doi:10.1029/2005WR004661.
Jordan, P., Seed, A., Austin, G., 2000. Sampling errors in radar estimates of rainfall. J. Geophys. Res. – Atmos. 105, 2247–2257.
Kavetski, D., Franks, S.W., Kuczera, G., 2002. Confronting input uncertainty in environmental modelling. In: Duan, Q., Gupta, H.V., Sorooshian, S., Rousseau, A.N., Turcotte, R. (Eds.), Calibration of Watershed Models. Water Science and Application, vol. 6. American Geophysical Union, pp. 49–68.
Kavetski, D., Kuczera, G., Franks, S.W., 2006a. Bayesian analysis of input uncertainty in hydrological modeling: 1. Theory. Water Resour. Res. 42 (3). doi:10.1029/2005WR00436.
Kavetski, D., Kuczera, G., Franks, S.W., 2006b. Bayesian analysis of input uncertainty in hydrological modeling: 2. Application. Water Resour. Res. 42, W03408. doi:10.1029/2005WR004376.
Komma, J., Bloschl, G., Reszler, C., 2008. Soil moisture updating by Ensemble Kalman Filtering in real-time flood forecasting. J. Hydrol. 357 (3–4), 228–242.
Krajewski, W.F., Smith, J., 2002. Radar hydrology: rainfall estimation. Adv. Water Resour. 25 (8–12), 1387–1394.
Kuczera, G., Kavetski, D., Franks, S., Thyer, M., 2006. Towards a Bayesian total error analysis of conceptual rainfall–runoff models: characterising model error using storm-dependent parameters'. J. Hydrol. 331, 161–177.
La Barbera, P., Lanza, L.G., Stagi, L., 2002. Influence of systematic mechanical errors of tippingbucket rain gauges on the statistics of rainfall extremes. Water Sci. Technol. 45 (2), 1–9.
Liang, X., Lettenmaier, D.P., Wood, E.F., 1996. One-dimensional statistical dynamic representation of subgrid spatial variability of precipitation in the two-layer variable infiltration capacity model. J. Geophys. Res. – Atmos. 101 (16), 21403–21422.
Liu, Y., Gupta, H.V., 2007. Uncertainty in hydrologic modeling: towards an integrated data assimilation framework. Water Resour. Res..
Lyon, S.W., Desilets, S.L.E., Troch, P.A., 2008. Characterizing the response of a catchment to an extreme rainfall event using hydrometric and isotopic data. Water Resour. Res. 44, W06413. doi:10.1029/2007WR006259.
Mandapaka, P.V., Krajewski, W.F., Ciach, G.J., Villarini, G., Smith, J.A., 2009. Estimation of radar-rainfall error spatial correlation. Adv. Water Resour. 32, 1020–1030.
Martinez-Fernandez, J., Ceballos, A., 2005. Mean soil moisture estimation using temporal stability analysis. J. Hydrol. 312, 28–38.
Molini, A., La Barbera, P., Lanza, L.G., Stagi, L., 2001. Rainfall intermittency and the sampling error of tipping-bucket rain gauges. Phys. Chem. Earth (C) 26 (10–12), 737–742.
Moradkhani, H., Hsu, K.-L., Gupta, H.V., Sorooshian, S., 2005a. Uncertainty assessment of hydrologic model states and parameters: sequential data assimilation using the particle filter. Water Resour. Res. 41. doi:10.1029/2004WR003604.
Moradkhani, H., Sorooshian, S., Gupta, H.V., Houser, P., 2005b. Dual state parameter estimation of hydrologic models using ensemble Kalman filter. Adv. Water Resour. 28, 135–147.
Moran, M.S., Stone, J.J., Renard, K.G., Heilman, P., Goodrich, D.C., Keefer, T.O., 2008. Preface to special section on fifty years of research and data collection: US Department of Agriculture Walnut Gulch Experimental Watershed. Water Resour. Res.. doi:10.1029/2007WR006083.
Morrissey, M.L., Maliekal, J.A., Greene, J.S., Wang, J., 1995. The uncertainty of simple spatial averages using rain gauge networks. Water Resour. Res. 31 (8), 2011–2017.
Moulin, L., Gaume, E., Obled, C., 2009. Uncertainties on mean areal precipitation: assessment and impact on streamflow simulations. Hydrol. Earth Syst. Sci. 13, 99–114.
Neuman, S.P., 2003. Maximum likelihood Bayesian averaging of uncertain model predictions. Stoch. Environ. Res. Risk Asses. 17, 291–305.
Nicol, J.C., 2001. High-Resolution Rainfall Measurements Using a Portable X-Band Radar System. Department of Physics, University of Auckland, Auckland.
Nicol, J.C., Austin, G.L., 2003. Attenuation correction constraint for single-polarisation weather radar. Meteorol. Appl. 10, 345–354.
North, G.R., 1987. Sampling studies for satellite estimation of rain. In: Preprints 10th Conf. on Probability and Statistics in Atmospheric Science, American Meteorological Society, Edmonton, pp. 129–135.
Pan, M., Wood, E.F., Wojcik, R., McCabe, M.F., 2008. Estimation of regional terrestrial water cycle using multi-sensor remote sensing observations and data assimilation. Remote Sens. Environ. 112 (4), 1282–1294.
Pauwels, V.R.N., De Lannoy, G.J.M., 2006. Improvement of modeled soil wetness conditions and turbulent fluxes through the assimilation of observed discharge. J. Hydrometeorol. 7 (3), 458–477.
Refsgaard, J.C., van der Sluijs, J.P., Brown, J., van der Keur, P., 2006. A framework for dealing with uncertainty due to model structure error. Adv. Water Resour. 29, 1586–1597.
Reichert, P., Mieleitner, J., 2009. Analyzing input and structural uncertainty of nonlinear dynamic models with stochastic, time-dependent parameters. Water Resour. Res. 45, W10402. doi:10.1029/2009WR007814.
Reichle, R.H., Walker, J.P., Koster, R.D., Houser, P.R., 2002. Extended versus ensemble Kalman filtering for land data assimilation. J. Hydrometeorol. 3 (6), 728–740.
Renard, B., Kavetski, D., Kuczera, G., Thyer, M., Franks, S.W., 2010. Understanding predictive uncertainty in hydrologic modeling: the challenge of identifying input and structural errors. Water Resour. Res. 46, W05521. doi:10.1029/2009WR008328.
Rodríguez-Iturbe, I., Mejía, J.M., 1974. The design of rainfall networks in time and space. Water Resour. Res. 10 (4), 713–728.
Shedekar, V., Brown, L., Heckel, M., King, K., Fausey, N., Harmel, R., 2009. Measurement errors in tipping bucket rain gauges under different rainfall intensities and their implication to hydrologic models. In: Proc 7th World Congress of Computers in Agriculture and Natural Resources, Available from American Society of Agricultural and Biological Engineers, St. Joseph, Michigan.
Steiner, M., 1996. Uncertainty of estimates of monthly areal rainfall for temporally sparse remote observations. Water Resour. Res. 32, 373–388.
Steiner, M., Bell, T.L., Zhang, Y., Wood, E.F., 2003. Comparison of two methods for estimating the sampling-related uncertainty of satellite rainfall averages based on a large radar dataset. J. Climate 16, 3759–3778.
Steinskog, D.J., Tjostheim, D.B., Kvamsto, N.G., 2007. A cautionary note on the use of the Kolmogorov–Smirnov test for normality. Monthly Weather Rev. 135, 1151–1157.
Sun, X., Mein, R.G., Keenan, T.D., Elliott, J.F., 2000. Flood estimation using radar and raingauge data. J. Hydrol. 239, 4–18.
Thiemann, T., Trosset, M., Gupta, H., Sorooshian, S., 2001. Bayesian recursive parameter estimation for hydrologic models. Water Resour. Res. 37 (10), 2521–2535.
Thyer, M., Renard, B., Kavetski, D., Kuczera, G., Franks, S.W., Srikanthan, S., 2009. Critical evaluation of parameter consistency and predictive uncertainty in hydrological modeling: a case study using Bayesian total error analysis. Water Resour. Res. 45, W00B14. doi:10.1029/2008WR006825.
Turner, M.R.J., Walker, J.P., Oke, P.R., 2008. Ensemble member generation for sequential data assimilation. Remote Sens. Environ. 112 (4), 1421–1433.
Vachaud, G., Passerat de Silans, A., Balabanis, P., Vauclin, M., 1985. Temporal stability of spatially measured soil water probability density function. Soil Sci. Soc. Am. J. 49, 822–828.
Villarini, G., Krajewski, W.F., 2008. Empirically-based modeling of spatial sampling uncertainties associated with rainfall measurements by rain gauges. Adv. Water Resour. 31 (7), 1015–1023.
Villarini, G., Mandapaka, P., Krajewski, W., Moore, R., 2008. Rainfall and sampling uncertainties: a rain gauge perspective. J. Geophys. Res. 113, D11102.12. doi:10.1029/2007JD009214.
Villarini, G., Krajewski, W.F., Ciach, G.J., Zimmerman, D.L., 2009. Product-error-driven generator of probable rainfall conditioned on WSR-88D precipitation estimates. Water Resour. Res. 45, W01404. doi:10.1029/2008WR006946.
Vrugt, J.A., Diks, C.G.H., Gupta, H.V., Bouten, W., Verstraten, J.M., 2005. Improved treatment of uncertainty in hydrologic modeling: combining the strength of global optimization and data assimilation. Water Resour. Res. 41, W01017–551561. doi:10.1029/2004WR003059.
Villarini, G., Krajewski, W.F., 2010. Review of the different sources of uncertainty in single-polarization radar-based estimates of rainfall. Surv. Geophys. 31, 107–129.
Volkmann, T.H.M., Lyon, S.W., Gupta, H.V., Troch, P.A., 2010. Multi-criteria design of rain gauge networks for flash flood prediction in semiarid catchments with complex terrain. Water Resour. Res. 46, W1554. doi:10.1029/2010WR007145.
Vrugt, J.A., Gupta, H.V., Bastidas, L.A., Bouten, W., Sorooshian, S., 2003a. Effective and efficient algorithm for multiobjective optimization of hydrologic models. Water Resour. Res. 39 (8). doi:10.1029/2002WR001746.
Vrugt, J.A., Gupta, H.V., Bouten, W., Sorooshian, S., 2003b. A shuffled complex evolution metropolis algorithm for optimization and uncertainty assessment of hydrologic model parameters. Water Resour. Res. 39 (8), 1201. doi:10.1029/2002WR001642.
Wagener, T., McIntyre, N., Lees, M.J., Wheater, H.S., Gupta, H.V., 2003. Towards reduced uncertainty in conceptual rainfall–runoff modeling: dynamic identifiability analysis. Hydrol. Processes 17, 455–476.
Wagener, T., Gupta, H.V., Yatheendradas, S., Goodrich, D., Unkrich, C., Schaffner, M., 2007. Understanding sources of uncertainty in flash-flood forecasting for semi-arid regions. In: Boegh, E., Kunstmann, H., Wagener, T., Hall, A., Bastidas, L., Franks, S., Gupta, H.V., Rosbjerg, D., Schaake, J. (Eds.), Quantification and Reduction of Predictive Uncertainty for Sustainable Water Resources Management. IAHS Redbook Publ. No. 313, pp. 204–212.
Woods, R.A., Grayson, R.B., Western, A.W., Duncan, M.J., Wilson, D.J., Young, R.I., Ibbitt, R.P., Henderson, R.D., McMahon, T.A., 2001. Experimental design and initial results from the Mahurangi River variability experiment: MARVEX. In: Lakshmi, V., Albertson, J.D., Schaake, J. (Eds.), Observations and Modelling of Land Surface Hydrological Processes. Water Resources Monographs, American Geophysical Union, Washington, DC, pp. 201–213.
Yatheendradas, S., Wagener, T., Gupta, H.V., Unkrich, C., Goodrich, D., Schaffner, M., Stewart, A., 2008. Understanding uncertainty in distributed flash-flood forecasting for semi-arid regions. Water Resour. Res. 44, W05S19. doi:10.1029/2007WR005940 (special issue on Walnut Gulch Experimental Watershed).
Young, C.B., Nelson, B.R., Bradley, A.A., Smith, J.A., Peters-Lidard, C.D., Kruger, A., Baeck, M.L., 1999. An evaluation of NEXRAD precipitation estimates in complex terrain. J. Geophys. Res. – Atmos. 104, 19691–19703.